RNA-based affinity purification reveals 7SK RNPs with distinct composition and regulation

J. Robert Hogg and Kathleen Collins

RNA published online Apr 24, 2007;
Access the most recent version at doi:10.1261/rna.565207

RNA-based affinity purification reveals 7SK RNPs with distinct composition and regulation

J. ROBERT HOGG[1] and KATHLEEN COLLINS

Department of Molecular and Cell Biology, University of California at Berkeley, Berkeley, California 94720-3200, USA

ABSTRACT

Recent studies have uncovered an unanticipated diversity of noncoding RNAs (ncRNAs), although these studies provide limited insight into their biological significance. Numerous general methods for identification and characterization of protein interactions have been developed, but similar approaches for characterizing cellular ncRNA interactions are lacking. Here we describe RNA Affinity in Tandem (RAT), an original, entirely RNA tag-based method for affinity purification of endogenously assembled RNP complexes. We demonstrate the general utility of RAT by isolating RNPs assembled in vivo on ncRNAs transcribed by RNA polymerase II or III. Using RAT in conjunction with protein identification by mass spectrometry and protein–RNA interaction assays, we define and characterize previously unanticipated protein subunits of endogenously assembled human 7SK RNPs. We show that 7SK RNA resides in a mixed population of RNPs with different protein compositions and responses to cellular stress. Depletion of a newly identified 7SK RNP component, hnRNP K, alters the partitioning of 7SK RNA among distinct RNPs. Our results establish the utility of a generalizable RNA-based RNP affinity purification method and provide insight into 7SK RNP dynamics.

Keywords: 7SK; U17; B2; *Pseudomonas* phage 7 coat protein; tobramycin aptamer

INTRODUCTION

Recently, thousands of putative ncRNA genes have been identified by cloning and computational efforts in many organisms (Costa 2005; Huttenhofer and Vogel 2006). An even greater diversity of ncRNA transcripts has been detected by genome tiling microarrays (Bertone et al. 2005). Although ncRNAs should be underrepresented in phenotype-based genetic screens, several ncRNA gene mutations have been recognized to cause human diseases including cartilage–hair hypoplasia and anauxetic dysplasia (Ridanpaa et al. 2001; Thiel et al. 2005), dyskeratosis congenita and aplastic anemia (Vulliamy et al. 2001, 2002), and cancer (Hammond 2006). Most ncRNAs, however, have unknown biological significance. Primary sequence analysis of ncRNA does not provide the functional insight that is routinely gained from sequence-based predictions of protein structure and interaction partners. For this reason, exploratory studies of recently discovered ncRNAs have focused on new members of previously characterized ncRNA families (Huttenhofer and Vogel 2006; Mattick and Makunin 2006). Future progress in understanding the general biological significance of ncRNAs will require new methods for functional analysis, including the identification of ncRNA interaction partners in vivo.

Ancestral catalytic RNAs are thought to have functioned without the aid of proteins, but their contemporary counterparts exploit the advantages of incorporation into ribonucleoprotein (RNP) complexes (Noller 2004; Walker and Engelke 2006). Proteins govern ncRNA processing, accumulation, localization, and activities; therefore, knowledge of the proteins associated with an ncRNA will inform hypotheses for its function. Endogenous RNP assembly typically involves a complex series of steps aided by chaperones, subcellular compartmentalization, and other factors (Schroeder et al. 2004). Because it is not generally possible to recapitulate in vitro the biological specificity conferred by these elaborate pathways (Singh and Valcarcel 2005), the physiological protein partners of an ncRNA are best determined by RNP reconstitution in vivo.

Building knowledge of the mechanisms of ncRNA function and RNP assembly will require generalizable methods for purification of endogenously assembled RNPs. Because

[1]**Present address:** Hammer Health Sciences Center, Columbia University, New York, NY 11032, USA.

Reprint requests to: Kathleen Collins, Department of Molecular and Cell Biology, University of California at Berkeley, Berkeley, CA 94720-3200, USA; e-mail: kcollins@berkeley.edu; fax: (510) 643-6971; J. Robert Hogg, Hammer Health Sciences Center, Columbia University, New York, NY 11032, USA; e-mail: jh2721@columbia.edu.

Article published online ahead of print. Article and publication date are at http://www.rnajournal.org/cgi/doi/10.1261/rna.565207.

many ncRNAs lack known protein-binding partners, we sought to develop an entirely RNA-based strategy for RNP affinity purification. Some RNPs can be enriched from cell extracts by hybridization of the RNA component with a complementary oligonucleotide (Lamond and Sproat 1994; Lingner and Cech 1996). This method has technical limitations imposed by the need for duplex formation by a previously single-stranded region of the RNA, which tends to destabilize RNP architecture. Instead, we focused on the use of RNA tags for affinity purification because small, structured RNA motifs can fold independently of a tagged RNA and bind to specific ligands with high affinity.

To date, RNA affinity tags have not been used successfully for unbiased discovery of protein subunits of endogenously assembled RNPs. Existing RNA tags can be classified into two categories. Tags in the first category were developed based on RNA–protein interactions found in nature. RNA motifs bound by MS2 phage coat protein or λ phage N anti-terminator protein are prominent examples of this type (Bardwell and Wickens 1990; Czaplinski et al. 2005). Tags in the second category were developed from aptamers evolved in vitro to possess affinity for specific ligands such as streptavidin, streptomycin, or tobramycin (Bachler et al. 1999; Srisawat and Engelke 2001; Hartmuth et al. 2002). Both types of tag have been used to recover proteins associated with RNAs transcribed and assembled into RNP in vitro, for example, in the characterization of spliceosomal complexes (Das et al. 2000; Hartmuth et al. 2002, 2004; Jurica and Moore 2002; Zhou et al. 2002). In these approaches, efficient RNP recovery can require the immobilization of tagged transcripts on resin prior to incubation with extract (Hartmuth et al. 2002, 2004; Granneman et al. 2004). Previous efforts to use RNA tags for isolation of RNPs assembled in vivo have provided only partial purification (Srisawat and Engelke 2001, 2002). Additional steps of purification dependent on prior knowledge of RNP properties have been required to identify novel proteins associated with tagged RNAs expressed in vivo (Watkins et al. 2000; Liang and Fournier 2006).

The 7SK RNA has emerged as an important regulator of the P-TEFb kinase (Nguyen et al. 2001; Yang et al. 2001; Blencowe 2002). Composed of cyclin-dependent kinase 9 (CDK9) and cyclin T1, T2 or K, P-TEFb phosphorylates the C-terminal domain (CTD) of RNA polymerase II (Pol II) to promote transcription elongation (Peterlin and Price 2006). About half of the cellular pool of P-TEFb is inhibited by binding to 7SK RNA and HEXIM proteins under normal growth conditions. While this aspect of 7SK RNA function is a subject of intense study, major questions persist. Importantly, estimates suggest that at most 30% of the cellular 7SK RNA pool assembles with P-TEFb and HEXIM proteins (Michels et al. 2003; Yik et al. 2003). Therefore, the proteins associated with the majority pool of 7SK RNPs are unknown. Furthermore, although 7SK RNA retains little or no association with P-TEFb or HEXIM proteins under stress conditions, stress does not dramatically impact the cellular accumulation level of 7SK RNA (Yang et al. 2001; Sano et al. 2002). These observations suggest that 7SK RNA assembles with proteins other than the known RNP components under both steady-state and stress conditions. Additional investigation of known 7SK RNP components may not be sufficient to reveal the composition and function of the putative alternative form(s) of 7SK RNP.

We have developed RNA Affinity in Tandem (RAT), an efficient and generalizable method for affinity purification of RNPs assembled in vivo. We show that RAT can isolate an endogenous RNP pool of mixed protein composition that could not have been isolated by affinity purification based on any individual RNP protein. We expressed RAT-tagged 7SK RNA in vivo, allowing endogenous assembly of the tagged RNA into RNPs, and purified tagged RNPs from whole cell extract. Proteins specifically associated with RAT-tagged 7SK RNA were identified by mass spectrometry. In marked contrast to the P-TEFb and HEXIM proteins of the known 7SK RNP, a set of newly identified 7SK RNP proteins interacts with 7SK RNA under both normal and cellular stress conditions. RNAi-mediated knockdown of one of these proteins, hnRNP K, indicates that it is important for the maintenance of a population of 7SK not bound to P-TEFb. Our findings establish the feasibility and general utility of using tandem RNA tags for purification of endogenously assembled RNPs, shed new light on 7SK RNP remodeling, and suggest new roles for 7SK RNA in transcriptional regulation.

RESULTS

RNA tags for RNP affinity purification

We sought to develop a method for isolation of endogenously assembled RNPs that employs only nondisruptive, RNA-based steps of purification. An extensive panel of previously tested and new candidate RNA tags was screened using criteria including biological stability when expressed in fusion with an ncRNA, high affinity for ligand at physiological ionic strength, and minimal competition by nonspecific interactions formed in complex cell extracts. We tested combinations of tags in sequential steps of purification, optimizing for efficient recovery and for both protein and RNA enrichment relative to contaminants. We found that the biological specificity of a naturally occurring RNA–protein interaction was required for optimal yield and enrichment in the first step. Disruption of this strong association required noncompetitive elution. The second step of purification could then employ an aptamer tag permissive for competitive elution by a small-molecule ligand.

The optimized RAT tag is composed of two hairpin stem–loops (Fig. 1A). The interaction of *Pseudomonas aeruginosa* phage 7 (PP7) coat protein with its cognate binding site

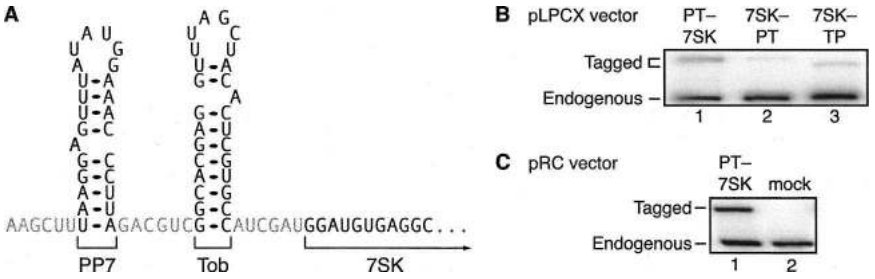

FIGURE 1. Expression of RAT-tagged 7SK RNAs. (*A*) RAT-7SK RNA. The 5′ end of human 7SK RNA was tagged with hairpins that bind PP7 coat protein (PP7) and tobramycin (Tob) as shown. (*B*) Various RAT-tagged 7SK RNAs were expressed using the human U6 RNA gene promoter subcloned into the vector backbone of pLPCX without the CMV promoter and polyadenylation signal. 7SK RNA was 5′ tagged with the PP7 hairpin followed by the tobramycin aptamer (PT-7SK) or 3′ tagged with the hairpins in either possible orientation (7SK-PT, 7SK-TP). Endogenous and recombinant 7SK RNAs were detected by Northern blot hybridization using total RNA from transiently transfected 293T cells. Transfection efficiency was routinely >70% (data not shown). (*C*) The PT-7SK RNA expression cassette was also subcloned into the vector backbone of pRc/CMV without the CMV promoter and polyadenylation signal. Endogenous and recombinant 7SK RNAs were detected as in *B*.

To demonstrate the general utility of RAT for isolation of endogenously assembled RNPs, we expressed tagged versions of several different ncRNAs, performed the two RNA-based steps of affinity purification of RNP from crude extracts, and examined the proteins that specifically copurified with each tagged RNA by SDS-PAGE. In addition to the human 7SK RNA described in greater detail below (Figs. 1, 2), we purified human U17 small nucleolar RNA transcribed by Pol II (Fig. 3A) and mouse transposon-derived B2 RNA transcribed by Pol III (Fig. 3B). These three ncRNAs have different biogenesis pathways and different functions, and correspondingly they copurified distinct sets of associated proteins.

provides the first purification step. This represents the first use of PP7 coat protein (PP7CP) as a binding partner for an RNA tag. Previous in vitro studies of RNA binding by PP7CP indicated that the interaction has a broader tolerance for variations in buffer ionic strength and pH than the more familiar MS2 coat protein–RNA interaction (Carey and Uhlenbeck 1983; Lim et al. 2001; Lim and Peabody 2002). Indeed, we achieved much higher RNP yield and enrichment with PP7 components than with the analogous components from MS2, particularly when using buffer conditions above minimal ionic strength (data not shown). A dimer of coat protein binds to a single RNA hairpin; coat protein dimers multimerize to form a phage capsid. We designed and screened sequence variants of PP7CP to obtain a recombinant protein with high RNA binding affinity but little if any dimer aggregation into multimers, aided by the previously determined PP7 capsid structure and studies of MS2 coat protein (LeCuyer et al. 1995; Tars et al. 2000). The optimized PP7CP (see Materials and Methods) was overexpressed in *Escherichia coli* as an N-terminal fusion to two Protein A domains (ZZ), with an intervening linker for cleavage by tobacco etch virus (TEV) protease (ZZ-tev-PP7CP). For the second step of RAT, we used an aptamer selected for binding to the aminoglycoside antibiotic tobramycin (Wang and Rando 1995; Hartmuth et al. 2004).

Purification of RAT-tagged 7SK RNPs

Human 7SK RNA is recovered in association with P-TEFb and HEXIM proteins, but the majority of this RNA is proposed to associate with other, unknown proteins. To

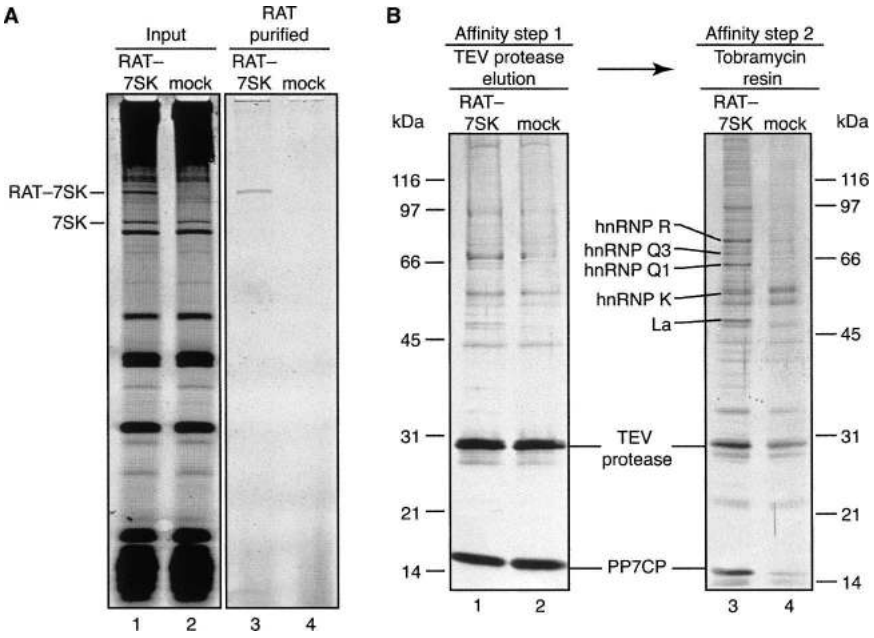

FIGURE 2. RAT purification of 7SK RNPs. (*A*) Purification of RAT-7SK RNA. Extracts from cells transiently transfected to express RAT-7SK or from untransfected cells were used for parallel affinity purifications. RNA was isolated from input whole cell extracts (lanes *1*,*2*) or washed tobramycin resin (lanes *3*,*4*), fractionated by denaturing PAGE, and visualized by staining with SYBR Gold. (*B*) Proteins in the TEV protease elution (lanes *1*,*2*) or bound to washed tobramycin resin (lanes *3*,*4*) from RAT-7SK RNA and mock purifications were resolved by SDS-PAGE and visualized by silver staining. Putative protein assignments are based on correlations to expected mobilities of proteins identified by mass spectrometry. All samples, including markers, were resolved on the same gel.

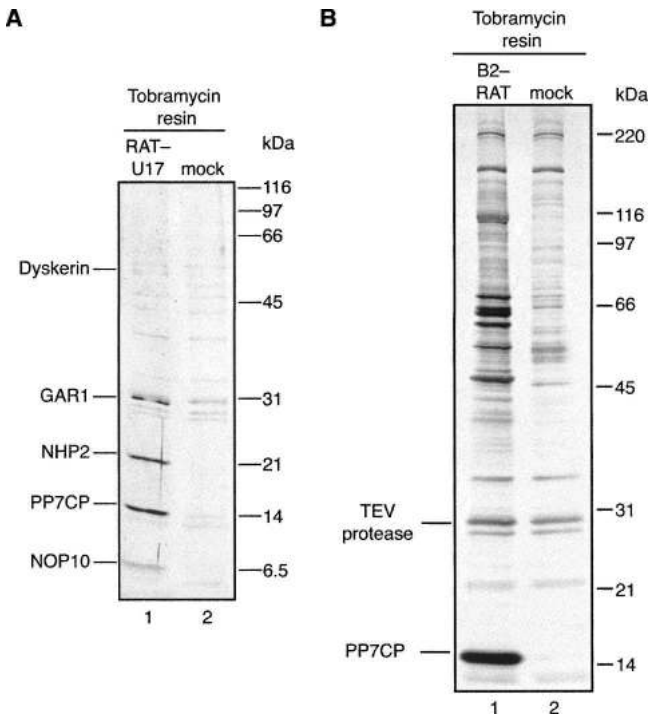

FIGURE 3. RAT purification of U17 and B2 RNPs. (*A*) The human U17 small nucleolar RNA, a member of the H/ACA-motif family of snoRNAs responsible for processing of the ribosomal RNA precursor (Eliceiri 2006), was tagged at the 5′ end with hairpins in the PT order. One-tenth of the material bound to washed tobramycin resin was used for SDS-PAGE and silver staining. The remaining nine-tenths were used for protein identification by mass spectrometry, which confirmed the presence of the core H/ACA-motif binding proteins dyskerin, GAR1, NHP2, and NOP10 specifically in the RAT-U17 purification. Silver staining of dyskerin was less intense than expected in relation to the other H/ACA-motif binding proteins, but dyskerin peptide sequences were not fewer than expected in relation to the other proteins in the mass spectrometry results, suggesting that silver staining intensity was unequal across this gel. (*B*) The SINE-encoded mouse B2 RNA, which has been suggested to inhibit Pol II transcription in response to cellular stress (Allen et al. 2004; Espinoza et al. 2004), was tagged at the 3′ end with hairpins in the PT order.

investigate the composition of the entire cellular pool of 7SK RNPs, we created expression constructs for RAT-tagged human 7SK RNA with hairpins in either relative orientation at the 5′ or 3′ end of 7SK RNA. We compared the accumulation of RAT-tagged 7SK RNAs following transient transfection of human 293T cells. The 5′-tagged RNA with the PP7 hairpin preceding the tobramycin aptamer accumulated to the highest level (Figs. 1A,B) and was used in subsequent experiments. Importantly, the accumulation level of RAT-7SK RNA did not exceed the level of endogenous untagged 7SK RNA when expressed from either of two vector backbone contexts (Figs. 1B,C). As preliminary evidence for physiologically relevant assembly of RAT-7SK RNA, we confirmed that tagged and untagged 7SK RNPs fractionated by gel filtration with similar profiles (data not shown). The biological accumulation and RNP assembly of RAT-tagged 7SK RNA, combined with more direct evidence for the physiological relevance of RAT-7SK RNP complexes described below, suggests that a RAT tag placed 5′ of the 7SK RNA did not prevent physiologically relevant RNP assembly in vivo.

We used whole cell extracts from human 293T cells expressing RAT-7SK RNA for tandem affinity purification. In parallel, we always performed a mock purification from cell extracts lacking tagged RNA as a control. Whole cell extracts were first supplemented with ZZ-tev-PP7CP. The coat protein and associated RNPs were recovered on IgG agarose and eluted from washed resin by addition of TEV protease. In the second purification step, tagged RNPs were enriched by binding to agarose derivatized with tobramycin. Elution was achieved by addition of free tobramycin as previously described (Hartmuth et al. 2002, 2004) or by elevation of the buffer pH or denaturation (this study). Over the course of numerous RNP affinity purifications (additional data not shown; Figs. 2, 3), we have not detected a common background of eukaryotic protein bound to the tag hairpins rather than to the unique ncRNA of interest. This is consistent with the fact that tag hairpins must be free to bind the exogenous PP7CP and tobramycin ligands used for affinity purification.

We investigated the complexity of RNAs in input extracts and purified samples by direct staining. RNAs in a sample were resolved by denaturing acrylamide gel electrophoresis and then detected by SYBR Gold. As expected, the input whole cell extracts harbored a diverse collection of RNAs (Fig. 2A, lanes 1,2). Following RAT, a single prominent RNA with the mobility of tagged 7SK RNA was detected only in the RAT-7SK RNA sample (Fig. 2A, lanes 3,4). Enrichment from nonspecific RNA contaminants was accomplished almost entirely by the first purification step, which reproducibly recovered >50% of the tagged RNA (data not shown). The second, tobramycin aptamer-based purification step was not as selective for tagged RNA relative to RNA contaminants. Overall tagged RNA recovery through two purification steps was 20%–30% of the input (data not shown).

Proteins present following the first or second step of RAT purification were detected by SDS-PAGE and silver staining. After elution from IgG agarose in the first step of purification, some polypeptides unique to the RAT-7SK RNA sample could be discerned, but overall the protein profiles of RAT-7SK RNA and mock samples were similar (Fig. 2B, lanes 1,2). At this stage, the most abundant proteins in both samples were TEV protease and PP7CP. The second purification step reduced nonspecific protein background, allowing additional proteins present specifically in the RAT-7SK RNA sample to be visualized (Fig. 2B, lanes 3,4). As expected, tobramycin resin enriched for PP7CP in a manner dependent on the tagged RNA. Together, these results demonstrate that RAT can isolate a tagged ncRNA and its specifically associated proteins from the complex mixture of a whole cell extract.

Specificity of protein association with RAT-7SK RNA

To determine the identities of proteins recovered in the RAT-7SK RNA and mock affinity purifications, we eluted RNP complexes from tobramycin resin, digested the entire mixture with trypsin, and analyzed peptide sequences by mass spectrometry. Protein identifications from the RAT-7SK RNA and mock samples were compared, yielding a list of proteins specific to the tagged ncRNA sample (Table 1). None of the five proteins specific to the RAT-7SK RNA sample identified by four or more peptide sequences was previously suggested to be in a 7SK RNP. Three of these new proteins were initially characterized in association with heterogeneous nuclear (hn) RNA: hnRNP K, hnRNP H, and hnRNP R (Krecic and Swanson 1999). In addition, hnRNP Q, a protein sharing >80% identity with hnRNP R, was identified by two peptides. Two other proteins enriched by RAT-7SK purification were the cold shock domain protein A (CSDA), which has an established RNA-binding activity (Kohno et al. 2003), and an ~120-kDa protein of unknown function annotated as C9orf10. The general Pol III transcription termination and RNP biogenesis factor La was identified by three peptides, consistent with previous immunoprecipitation results (Rinke and Steitz 1982; Chambers et al. 1983; Wassarman and Steitz 1991). Cyclin T1 was identified by one peptide, indicating that some RAT-7SK RNA was assembled into the known P-TEFb RNP. The nonquantitative nature of mass spectrometry precludes any precise conclusion about the relative amounts of the newly identified proteins versus previously known proteins in the pool of isolated 7SK RNPs. However, less robust identification of proteins from the known RNP is consistent with observations that it has a minority and condition-dependent presence in the steady-state 7SK RNP pool (Michels et al. 2003; Yik et al. 2003).

We confirmed that known and newly identified 7SK RNP proteins were, indeed, enriched in the RAT-7SK RNA purification using an immunoblotting approach. As expected, antibodies against CDK9, cyclin T1, and HEXIM1 recognized proteins of appropriate sizes in whole cell extracts and in the 7SK RNP sample, but not in the mock sample purified in parallel. This provides evidence that RAT-tagged 7SK RNA was assembled into physiologically relevant RNPs (Fig. 4A,B). An antibody specific for the hnRNP Q/R proteins recognized polypeptides of four distinct sizes in whole cell extract (Fig. 4C), corresponding to hnRNP R (the largest protein) and three isoforms of hnRNP Q produced by alternative splicing (Mourelatos et al. 2001). At least three of these four polypeptides appeared enriched in the RAT-7SK purification, representing hnRNP R and two isoforms of hnRNP Q designated by relative mobility as hnRNP Q1 and hnRNP Q3. The intermediate-mobility hnRNP Q2 protein lacks a portion of the second RNA-binding RRM motif, which could reduce its association with 7SK RNA.

We also examined input extracts and purified samples using an antibody specific for hnRNP K. At least two sizes of hnRNP K were detected in whole cell extract (Fig. 4D). The smallest version of the protein is likely to derive from an exon-skipping event that results in removal of a portion of the protein between the first and second RNA-binding KH domains (Makeyev and Liebhaber 2002). The RAT-7SK RNP sample but not the mock sample contained hnRNP K, with enrichment for the smaller isoform. Quantitative immunoblot analysis indicated that the large isoforms of hnRNP K were fourfold more abundant than the small isoform in input extract but fourfold less abundant in purified 7SK RNPs. In reciprocal interaction assays (described below), we used tagged versions of two hnRNP K isoforms: one containing the alternatively spliced exon designated hnRNP K3 (GenBank accession NP_112553.1) and one lacking this exon designated hnRNP K4.

TABLE 1. Protein identification by mass spectrometry

Protein	Peptides	% coverage
All proteins identified by four or more peptides in RAT–7SK RNP		
hnRNP R	9	17
hnRNP H	6	15
hnRNP K	4	14
Cold shock domain protein A (CSDA)	4	12
C9orf10	4	6
7SK RNP proteins identified by three or fewer peptides		
La	3	10
hnRNP Q	2	4
Cyclin T1	1	4

Reciprocal protein-based affinity purification of untagged endogenous 7SK RNA

To examine the RNA interaction specificity of the proteins that copurified with RAT-tagged 7SK RNA, we assayed their ability to copurify endogenous untagged 7SK RNA. Tagged proteins were expressed under the control of the relatively weak promoter within the long terminal repeat of the pBABE retroviral vector (Morgenstern and Land 1990). We have found that tagged proteins expressed in this context by transient transfection of 293T cells typically accumulate at a level comparable to that of the endogenous protein (Fig. 5A, WCE + TEV protease lanes; see legend), rather than at the higher level that can be obtained by placing tagged protein expression under the control of a stronger promoter. Each protein was expressed in vivo as an N-terminal fusion to the tandem affinity purification (TAP) tag (Puig et al. 2001) and purified from whole cell extract using IgG agarose. To assay for interactions between these proteins and 7SK RNA under both normal and stress conditions, cells were treated prior to extract preparation

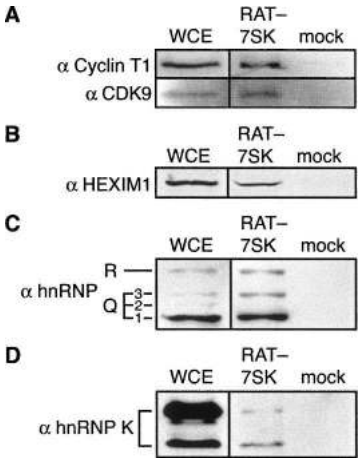

FIGURE 4. RAT purification specificity of candidate 7SK RNP proteins. Proteins in input whole cell extract (WCE) or bound to washed tobramycin resin of RAT-7SK or mock affinity purifications were used for immunoblots with the antibodies indicated.

with either the Pol II CTD kinase inhibitor 5,6-dichloro-1-β-D-ribofuranosylbenzimidazole (DRB), which disrupts the 7SK RNP containing P-TEFb and HEXIM proteins (Nguyen et al. 2001), or the carrier DMSO as a control. The 7SK RNA in input and bound samples was detected by Northern blot hybridization (Fig. 5B, top two panels), and the total RNA content of purified samples was examined by staining with SYBR Gold (Fig. 5B, bottom two panels).

Several of the tagged proteins showed high selectivity in their copurification of untagged endogenous 7SK RNA. Consistent with the results described above, we found that hnRNP R, hnRNP Q3, and hnRNP Q1 but not hnRNP Q2 copurified endogenous 7SK RNA above the background interaction monitored using control purifications from extracts of cells expressing the TAP tag alone (Fig. 5B, lanes 1–8 versus 17–18). Similarly, hnRNP K4 copurified endogenous 7SK RNA (Fig. 5B, lanes 9–12). TAP-tagged hnRNP K3 accumulated to a level severalfold lower than that of the endogenous protein when expressed using the pBABE vector context (Fig. 5A, lanes 11–16). If TAP-tagged hnRNP K3 accumulation was increased by using an expression vector with a stronger promoter, an interaction with endogenous 7SK RNA could be detected (data not shown). Unrelated TAP-tagged hnRNP proteins did not show a similar specificity of ncRNA interaction (data not shown).

TAP-tagged CSDA also copurified 7SK RNA (Fig. 5B, lanes 15,16), as well as a spectrum of other ncRNAs, suggesting that CSDA has less selectivity for 7SK RNA than the hnRNP proteins assayed in parallel (data not shown). TAP-tagged C9orf10 copurified a small amount of 7SK RNA (Fig. 5B, lanes 13,14) from cell extracts with almost undetectable levels of tagged protein (Fig. 5C, lanes 13,14). The atypically low accumulation levels of this recombinant protein preclude a firm conclusion about its RNA interaction specificity. We used antibody immunopurification to confirm the association of endogenous La with 7SK RNA and other Pol III transcripts (Fig. 6). Finally, TAP-tagged hnRNP H copurified endogenous 7SK RNA when expressed from a vector with a strong promoter but not when expressed using the pBABE vector (data not shown) and was not characterized in subsequent studies.

In addition to these tests of reciprocal interaction specificity using native cell extracts, we used extracts solubulized from formaldehyde cross-linked cells for immunopurification under stringent denaturing conditions. This approach is generally considered to capture only the RNA–protein associations existing in vivo prior to cell lysis (Niranjanakumari et al. 2002). Of the commercially available antibodies, an antibody against hnRNP K retained enough binding affinity to allow detection of associated RNA under the stringent conditions used for purification of cross-linked complexes. The purification of endogenous untagged hnRNP K from cross-linked cell extracts revealed a highly specific copurification of endogenous untagged 7SK RNA (Fig. 7).

Differential regulation of the 7SK RNPs by cellular stress

The 7SK RNP containing P-TEFb and HEXIM proteins dissociates under conditions considered to be forms of cellular stress (Nguyen et al. 2001; Yang et al. 2001; Sano et al. 2002; Michels et al. 2003; Yik et al. 2003). In agreement with previous studies, we found that treatment of cells with the CDK inhibitor DRB prior to cell lysis greatly reduced the amount of 7SK RNA recovered in association with cyclin T1 (Fig. 5B, lanes 19,20). In contrast, 7SK RNA copurification with other proteins was not diminished by DRB (Fig. 5B). In fact, DRB increased the amount of 7SK RNA recovered in association with hnRNP R, hnRNP Q3, and hnRNP K4 (Fig. 5B, lanes 5–10). Similar results were obtained if cells were treated with actinomycin D rather than DRB (data not shown). Both forms of stress also increased the amount of TAP-tagged hnRNP R, hnRNP Q3, and hnRNP K4 in whole cell extracts (Fig. 5C, lanes 5–10) without impact on the levels of numerous other TAP-tagged proteins (additional data not shown; Fig. 5C, lanes 1,2,11,12,15,16). The increase in accumulation of some tagged proteins is not due to a change in transfection efficiency but may be due in part to the transient expression context, because smaller changes were observed in the pool of endogenous proteins (data not shown).

The DRB-induced increase in 7SK RNA copurification with TAP-tagged hnRNP R, hnRNP Q3, and hnRNP K4 in DRB-treated cells could reflect the increase in protein accumulation levels. Alternatively, if the newly characterized 7SK RNP proteins are mutually exclusive with P-TEFb and HEXIM proteins in binding to 7SK RNA, P-TEFb and HEXIM protein dissociation may enhance their RNP incorporation. We used tagged proteins to examine the relationships among 7SK RNP proteins. A cyclin T1

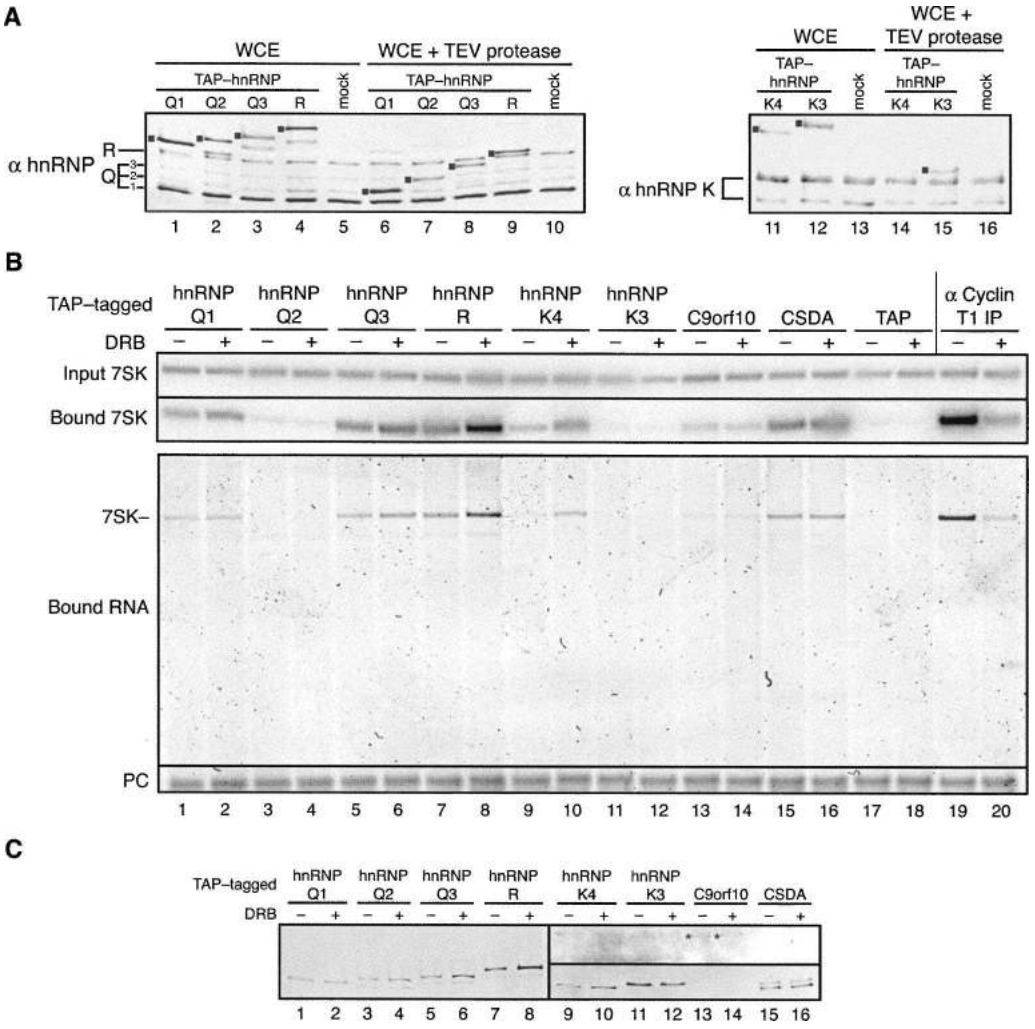

FIGURE 5. Protein associations with endogenous 7SK RNPs. (*A*) Endogenous and recombinant proteins were detected using antibodies against hnRNP Q/R (*left*) or hnRNP K (*right*). Endogenous hnRNP R, hnRNP Q isoforms, and hnRNP K isoforms are labeled. Primary antibody binding to the Protein A domains of the TAP tag amplifies the immunoblot signal of tagged proteins. However, this signal amplification can be eliminated by TEV protease cleavage between the Protein A domains and the calmodulin-binding peptide of the TAP tag. Protease-cleaved TAP-tagged hnRNP K4 is not evident due to its probable comigration with the larger isoform of endogenous hnRNP K. (*B*) TAP-tagged proteins in extracts of cells treated with DMSO alone (odd lanes) or DRB in DMSO (even lanes) were purified using IgG agarose. RNAs from input extracts were examined by Northern blot hybridization to detect 7SK RNA (*top* panel). RNAs bound to IgG agarose were examined by Northern blot hybridization to detect 7SK RNA (second panel from *top*) or stained with SYBR Gold following denaturing PAGE to detect endogenous RNAs (*large* panel) and the internal precipitation control (PC) added before RNA precipitation (*bottom* panel). Untransfected cell extract was used for immunopurification of cyclin T1 as a control (lanes *19*,*20*). (*C*) TAP-tagged proteins in the whole cell extracts used for purification in *B* were detected by immunoblotting with nonspecific rabbit IgG. Asterisks mark the position of recombinant C9orf10 protein (lanes *13*,*14*), which is equally but barely detectable in both lanes. The *upper* half of the blot is shown for lanes 9–16 as an overexposure relative to the *bottom* half to enable visualization of the C9orf10 signal.

antibody but not nonspecific IgG enriched CDK9 from cell extracts (Fig. 8A, lanes 1,2). However, purification of TAP-tagged hnRNP R, hnRNP K4, or CSDA recovered very low levels of CDK9 (Fig. 8A, lanes 3–6). Each of these purified samples contained a similar amount of 7SK RNA (Fig. 8A, right). In comparison, although the cyclin T1 antibody did not enrich hnRNP K or hnRNP Q (Fig. 8B, lanes 5,6,5′,6′), purification of TAP-tagged hnRNP R, hnRNP K4, and CSDA did (Fig. 8B, lanes 1–3,1′–3′). Each of these samples contained a comparable amount of 7SK RNA (Fig. 8B, right). These results are consistent with largely nonoverlapping protein composition of the previously characterized and newly identified 7SK RNPs.

hnRNP K depletion alters 7SK RNA distribution among RNPs

We used RNAi-mediated knockdown of hnRNP K to investigate the impact of protein depletion on 7SK RNPs. HeLa cells were transfected in triplicate with siRNA targeting

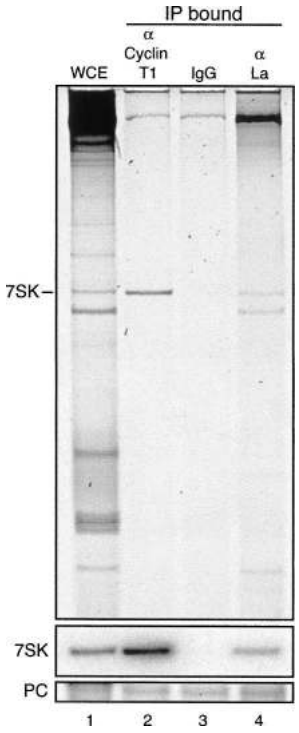

FIGURE 6. Immunopurification of cyclin T1 or La enriches 7SK RNA. Whole cell extract was incubated with immobilized antibodies against cyclin T1 or La or a nonspecific goat IgG control. RNA extracted from the input whole cell extract (lane *1*) and antibody-bound material (lanes *2–4*) was resolved by denaturing PAGE and detected by either SYBR Gold staining (*top* panel) or Northern blot hybridization for 7SK RNA (*center* panel). An internal tRNA precipitation control (PC) added during RNA extraction was visualized by SYBR Gold staining (*bottom* panel).

hnRNP K or negative control siRNA. We observed an ~40% reduction of the steady-state level of 7SK RNA upon hnRNP K depletion, as well as reduced abundance of several other ncRNAs (data not shown; U3 RNA was used as the normalization control). Whole cell extracts were adjusted to contain equal levels of 7SK RNA and used for immunoprecipitation with a cyclin T1 antibody. Extracts of hnRNP K-depleted cells consistently gave an elevated level of 7SK RNA copurification with cyclin T1 (Fig. 9A,B). Similar results were obtained using a second siRNA targeting hnRNP K, while no effect was observed following CSDA depletion (data not shown). The level of hnRNP K protein was reduced but not eliminated in these extracts (Fig. 9C). These results indicate that hnRNP K knockdown increased the proportion of 7SK RNA bound to P-TEFb.

In one simple model consistent with previous results and our findings above, 7SK RNA can assemble as two distinct multisubunit RNPs that exchange in a stress-regulated equilibrium (Fig. 9D). The depletion of individual 7SK RNP proteins can alter the distribution of 7SK RNA among these RNPs. The proteins associated with 7SK RNA could all bind RNA directly, as shown in Figure 9D, or some could assemble into RNP through protein–protein interactions. Also, the newly identified 7SK RNA-interacting proteins could combine to form a shared 7SK RNP, as shown in Figure 9D, or form separate RNPs. Future experiments will be necessary to more precisely define the complete list of 7SK RNP subunits and the protein architecture of alternative 7SK RNPs.

DISCUSSION

To our knowledge, the isolation of 7SK RNPs using RAT is the first entirely RNA tag-based affinity purification of endogenously assembled RNPs from crude cell extract to a homogeneity sufficient for identification of unknown associated proteins. RAT allows efficient and gentle affinity purification of RNPs under diverse buffer conditions. The utility of RAT is highlighted by the isolation of proteins that associate with 7SK RNA in a manner mutually exclusive with the association of P-TEFb and HEXIM proteins. Because the newly identified proteins assemble into 7SK RNPs lacking previously known protein subunits, an RNA-based affinity purification approach was essential to identify them.

The success of the RAT approach is largely derived from the optimized first step of affinity purification. In comparison to the interaction of MS2 coat protein with its cognate RNA, PP7CP has high affinity for its RNA-binding site

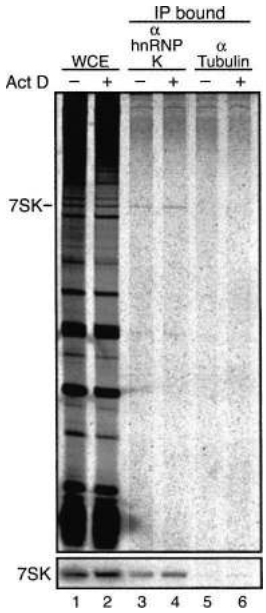

FIGURE 7. Cross-linking of hnRNP K to 7SK RNA in vivo. Untreated cells or cells treated with actinomycin D (Act D) were cross-linked with formaldehyde. Whole cell extracts (WCE) were prepared by sonication and immunopurified using antibodies against hnRNP K or tubulin. RNA in the WCE and antibody-bound fractions (IP bound) was resolved by denaturing PAGE and detected by either SYBR Gold staining (*top* panel) or Northern blot hybridization for 7SK RNA (*bottom* panel).

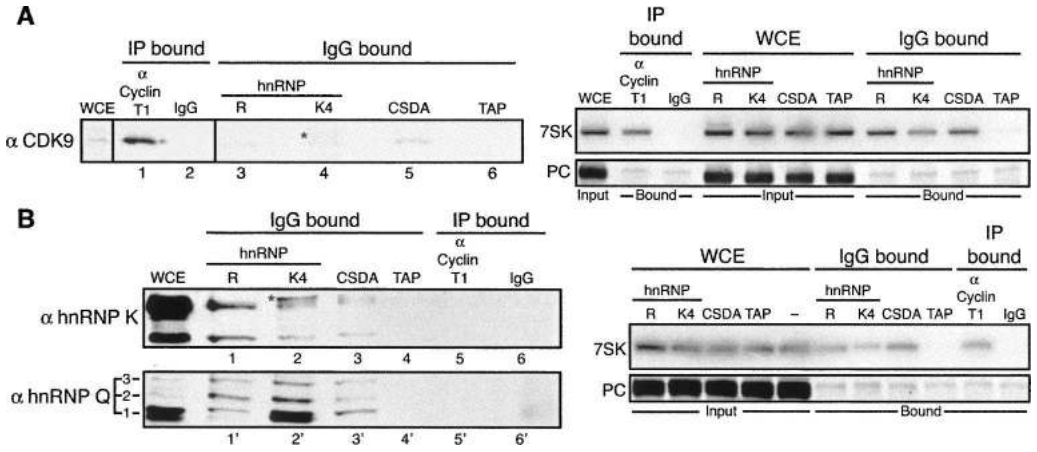

FIGURE 8. Distinct, potentially multi-subunit 7SK RNPs. Whole cell extracts from untransfected cells were used for immunoaffinity purification with cyclin T1 antibody or nonspecific IgG. Whole cell extracts from cells transfected to express TAP-tagged proteins or the TAP tag alone (TAP) from the pcDNA 3.1 vector backbone were used for affinity purification with IgG agarose. (At *right*) Part of the input and bound fractions was used to extract RNA for SYBR Gold staining of input and precipitation controls and Northern blot hybridization to detect 7SK RNA. (*A*) Complexes were eluted with 2% SDS and used for immunoblotting with an antibody against CDK9. The asterisk denotes signal from nonspecific cross-reaction with TAP-hnRNP K4 due to the tag Protein A domains. All of the samples shown were run on the same gel and imaged together using the same setting. (*B*) Complexes were eluted with HLB150 supplemented with 1 M urea, 0.5 M NaCl, and 0.05% SDS and used for immunoblotting with antibodies against hnRNP K or hnRNP Q/R. The asterisk denotes signal from signal from nonspecific cross-reaction with TAP-hnRNP K4 due to the tag Protein A domains. The copurification of hnRNP R is obscured by TAP-hnRNP K.

across a wider range of ionic strength and pH (Carey and Uhlenbeck 1983; Lim et al. 2001). The PP7CP–RNA interaction also seems relatively uncompromised by nonspecific competition from the large complexity of factors in crude cell extracts, allowing high yield and selectivity under nondisruptive conditions. Elution using TEV protease also adds to the extent of tagged RNP enrichment by selecting against proteins and RNAs that bind nonspecifically to IgG agarose. The aptamer-based purification step provides a third type of enrichment specificity. Binding to tobramycin resin removed protein background, most notably depleting the free PP7CP and TEV protease. We have found that other aptamer tags can be used successfully following a first step of PP7 tag purification and can be interchanged depending on the specificity of purification desired (data not shown). Overall, RAT shares the experimental logic of the successful protein TAP tag (Rigaut et al. 1999), which uses two Protein A domains for a first step of binding to IgG agarose, noncompetitive elution from IgG agarose by TEV protease, and a second purification step permissive for elution with a small molecule.

Previous studies have demonstrated that the 7SK RNP containing P-TEFb and HEXIM proteins is disassembled in response to cellular stress. Knowledge of the composition of the other forms of 7SK RNP is a prerequisite for understanding this physiologically important RNP remodeling event. The newly identified 7SK RNP proteins described here assemble with 7SK RNA at steady state and persist in their association with 7SK RNA during cellular stress. Because at least one form of RNP remains intact under stress, a dynamic equilibrium of RNP compositions would allow a constant level of 7SK RNA accumulation despite transient dissociation of the RNP containing P-TEFb and HEXIM proteins. The cellular events responsible for changing the balance of this equilibrium remain to be defined. We show that depletion of hnRNP K causes a decrease in 7SK RNA accumulation and a concomitant increase in the association of 7SK RNA with P-TEFb. An hnRNP K-bound reservoir of 7SK RNA distinct from the P-TEFb/HEXIM RNP could be crucial for rapid inhibition of P-TEFb in response to changes in cellular conditions.

The 7SK RNPs lacking P-TEFb may also play an autonomous cellular role. The biochemically distinct 7SK RNA-binding proteins characterized here were all previously implicated in transcriptional regulation. The hnRNP proteins were first characterized as general pre-mRNA-binding proteins, but it is increasingly clear that they also have specialized roles (Krecic and Swanson 1999). Intriguingly, the hnRNP Q/R proteins were isolated as direct, phosphorylation-dependent binding partners of the Pol II CTD (Carty and Greenleaf 2002). Also, hnRNP K was proposed to have roles in Pol II-mediated transcription based on evidence of associations with transcription machinery, transcription factors, and chromatin-remodeling complexes (Bomsztyk et al. 2004). The relationships between these previously described functions and 7SK RNA biology should be re-examined in light of the interactions identified here.

Future uses of RAT can exploit its unique ability to purify physiologically assembled RNP complexes to near homogeneity. A DNA sequence cassette containing the RAT tag can be inserted into recombinant RNA expression

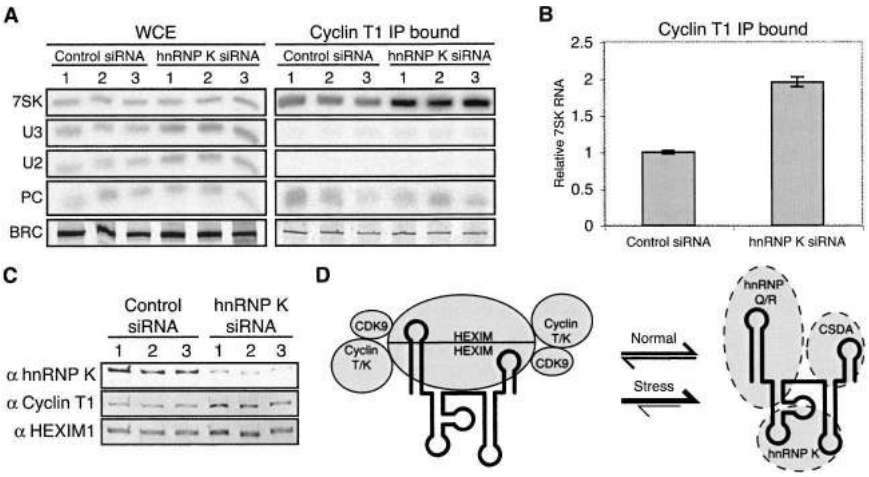

FIGURE 9. Effect of hnRNP K depletion on 7SK RNP assembly. (*A*) Whole cell extracts from cells transfected with hnRNP K or control siRNAs were used for immunoaffinity purification with a cyclin T1 antibody. RNAs from input and bound fractions were examined by Northern blot hybridization to detect the indicated RNAs and an oligonucleotide precipitation control (PC). The bead recovery control (BRC) was visualized by SYBR Gold staining. All samples were electrophoresed on the same gel, and identical settings were used to visualize WCE and bound signals for each RNA. (*B*) Quantification of data in *A*. 7SK RNA recovery was normalized to the precipitation control and input 7SK RNA levels. Error bars indicate the standard error of the mean from three independent samples. (*C*) Immunoblots of hnRNP K, cyclin T1, and HEXIM1 in the whole cell extracts used for purification in *A*. Note that control siRNA lanes have slightly less total protein than hnRNP K siRNA lanes. (*D*) Model for 7SK RNP compositions and their dynamics of exchange. P-TEFb and HEXIM proteins are illustrated in accord with previous studies (Li et al. 2005; Egloff et al. 2006). The relative placement of newly identified 7SK RNP proteins on a shared molecule of 7SK RNA is intended as an aid for visualization, not as a specific model of RNP structure.

vectors, as done here, or at endogenous ncRNA gene loci. RAT tag integration into ncRNA gene loci could afford an opportunity for high-throughput purification and characterization of a great diversity of ncRNA complexes. In addition, it may be possible to extend the RAT approach to isolate specific mRNAs or nascent RNA transcripts. The PP7 tag may also be useful for studying RNA subcellular localization through coexpression of hairpin-tagged RNA and fluorescent protein-tagged PP7CP (Shav-Tal et al. 2004). Because there is no cross-recognition in the binding specificity of the MS2 and PP7 coat proteins (Lim et al. 2001; Lim and Peabody 2002), differentially tagged RNAs could be localized in the same cell. Successful RNA tags for purification and visualization will facilitate the long-term process of deciphering new functions of this diverse class of evolutionarily significant biomolecules.

MATERIALS AND METHODS

Constructs

RAT tag cassettes were constructed from overlapping oligonucleotides. We used the wild-type PP7 hairpin sequence (Lim and Peabody 2002) and the J6 stem–loop tobramycin aptamer (Wang and Rando 1995). This tobramycin aptamer has a shorter stem and fewer bulged residues than the tobramycin aptamer previously used for affinity purification (Hartmuth et al. 2004). Plasmid pETP7CTNc encoding the PP7 coat protein (Lim et al. 2001) was a kind gift of David Peabody (University of New Mexico). The NcoI–BamHI fragment of pETP7CTNc and the ZZ-tev portion of the N-terminal TAP tag (Puig et al. 2001) were subcloned into pET28a (Novagen) in frame with the C-terminal $(His)_6$ tag to generate pETZZ-tev-PP7CP. Mutagenesis was performed on double-stranded DNA as described (Mitchell et al. 1999a) to create the C68A,C71A-modified coat protein with optimal RNA binding but reduced aggregation properties.

DNA fragments encoding human 7SK RNA (GenBank accession NR_001445) and a 284 base pair region of the human U6 RNA gene promoter were combined with a pRc/CMV (Invitrogen) or pLPCX (Clontech) plasmid backbone lacking the CMV promoter and polyadenylation signal. RAT-U17 RNA was expressed at near-endogenous levels following stable integration of the expression vector into the genome of 293T cells, with expression driven by the human U3 snoRNA gene promoter. B2-RAT RNA was expressed from its internal Pol III promoter by transient transfection of 293T cells. Constructs for human protein expression encoded N-terminally TAP-tagged fusion proteins and used the vector backbone of pBABE (Morgenstern and Land 1990) or pcDNA3.1 (Invitrogen) as indicated. Each open reading frame was amplified by RT-PCR using total RNA from 293T cells. All constructs were sequenced to confirm expression of the intended product.

RAT reagents

Recombinant PP7CP was expressed in the *E. coli* strain BL21 (DE3). Starter cultures were diluted 1:500 in 500 mL of 2xYT + 25 μg/mL kanamycin and grown at 37°C until reaching $OD600_{0.4–0.5}$, at which point 1 mM IPTG was added. Cells were harvested by centrifugation after 4 h of induction at 37°C. Pellets were resuspended in 20 mL of buffer with 20 mM Tris (pH 8.0), 1 mM $MgCl_2$, 10% glycerol, and protease inhibitors, then sonicated. Sonicates were adjusted to 200 mM NaCl, 20 mM imidazole, and 0.1% NP-40 and centrifuged at 18,000*g* for 20 min at 4°C. Supernatants were incubated with 0.5 mL of Ni-NTA resin (QIAGEN) for 1 h at 4°C, packed in polyprep columns (Bio-Rad), and washed with 20 mL of wash buffer (20 mM Tris at pH 8.0, 200 mM NaCl, 20 mM imidazole, 1 mM $MgCl_2$, 0.1% NP-40, 10% glycerol, protease inhibitors). Coat protein was eluted with wash buffer supplemented with 0.5 M imidazole, aliquoted, and snap frozen in liquid nitrogen.

Tobramycin (Sigma) was coupled to Affi-Gel 10 resin (Bio-Rad). Resin washed into water was resuspended in an equal volume of 20 mM HEPES (pH 7.5) and 100 mM tobramycin, rotated overnight at 4°C, and then supplemented with 100 mM ethanolamine (pH 8.0) for 2 h to block unreacted coupling sites.

Cell culture and extracts

We used the Phoenix line of 293T cells (Kinsella and Nolan 1996), which has superior growth properties and can be transfected with particularly high efficiency using calcium phosphate. Phoenix 293T cells were maintained in DMEM supplemented with 10% fetal calf serum and antibiotics. Transfection by calcium phosphate was performed as described (Mitchell et al. 1999a) in 15 cm (RAT purifications) or 10 cm plates. Where indicated, cells were treated with 50 μM DRB (Sigma) or 1 μg/mL actinomycin D (Sigma) for 1 h prior to extract preparation (Nguyen et al. 2001; Yang et al. 2001).

Whole cell extracts were prepared as previously described (Mitchell et al. 1999b) with minor modifications. Cells were resuspended in hypotonic lysis buffer (HLB) containing 20 mM HEPES (pH 7.9), 2 mM $MgCl_2$, 10% glycerol, 0.1% NP-40, 0.5 mM DTT, and 0.1 mM PMSF for lysis and subsequently extracted with 200 mM NaCl. For the nucleolar U17 RNP, cells were dounce-homogenized in hypotonic lysis buffer, and nuclei were purified prior to extract production. Extraction buffer was adjusted to 400 mM NaCl to effectively solubilize nucleolar complexes. Nuclear extract was clarified by centrifugation and then diluted to 200 mM NaCl prior to use for affinity purification.

RAT purification

All RAT purification steps were conducted at 4°C. Whole cell extracts from 1 to 15 plates of 293T cells were adjusted to 2.5 mg/mL protein in HLB with 150 mM NaCl, supplemented with 3.5 μg/mL ZZ-tev-PP7CP, and rotated for 60 min before addition of 20 μL/mL rabbit IgG agarose (Sigma) and 90 min of additional rotation. Resin was washed extensively in HLB150 and resuspended in an equal volume of HLB150 without NP-40. Coat protein was eluted from resin with 30 μg/mL TEV protease (Kapust et al. 2001) for 60 min. Elution supernatants were separated from resin using Micro BioSpin Columns (Bio-Rad). Resin was then rinsed with an equal volume of HLB150 without NP-40. The elution and rinse fractions were pooled, supplemented with 5 mM DTT, and combined with (3 μL of tobramycin resin)/(mL of starting extract) for 45 min. This resin was washed three times in HLB150 without NP-40. Bound material was eluted in 80% acetonitrile and 5% formic acid for electrophoresis.

Mass spectrometry

Elution from tobramycin resin was performed using 2.5 packed gel volumes of 100 mM ammonium carbonate (pH 10), which was subsequently dried by vacuum. Pellets were resuspended in 40 μL of 8 M urea in 100 mM Tris (pH 8.5), reduced in 5 mM Tris [2-carboxyethyl] phosphine (Pierce), carboxyamidated in 10 mM iodoacetamide (Sigma), diluted to 2 M urea in 100 mM Tris (pH 8.5), and digested with 0.5 μg of sequencing-grade trypsin (Promega). Peptides were purified on Spec PT C18 pipette tips (Varian). Mass spectrometry was performed on a Thermo Finnegan LCQ Deca XP Plus. Spectra were analyzed with the SEQUEST algorithm (Eng et al. 1994), and protein identifications in RAT-7SK RNA and mock purifications were compared using DTASelect and Contrast software (Tabb et al. 2002). The percent peptide coverage for each protein shown in Table 1 was estimated using DTASelect.

Protein-based affinity purification and detection of RNA and protein

Whole cell extracts containing TAP-tagged proteins were adjusted to 1–2 mg/mL protein in HLB150 and rotated with 5 μL of rabbit IgG agarose (Sigma) for 2 h at 4°C. Bound samples were washed extensively with cold HLB150. Cyclin T1 immunopurification used the same conditions with 5 μL of GammaBind G Sepharose (G.E. Biosciences) prebound with goat anti-cyclin T1 (T-18; Santa Cruz). RNA extraction was performed by the guanidine-acid phenol method (Ausubel et al. 1996). A tRNA or oligonucleotide precipitation control was added during RNA extraction as indicated. RNAs were separated on 6% or 9% acrylamide (19:1), 7 M urea, 0.6× TBE gels; stained with SYBR Gold (Invitrogen); and analyzed on the Typhoon 9400 using ImageQuant software (G.E. Biosciences). Northern blots were performed as described (Mitchell et al. 1999a) using end-labeled DNA oligonucleotides.

Phoenix 293T cells were cross-linked with formaldehyde as previously described (Niranjanakumari et al. 2002; Kaneko and Manley 2005), with modifications. Cells were cross-linked in 0.1% formaldehyde for 8 min at room temperature; washed; resuspended in 50 mM Tris (pH 7.4), 1% NP-40, 0.5% sodium deoxycholate, 0.05% SDS, 2 mM $MgCl_2$, and 150 mM NaCl; and sonicated three times for 20 sec each at power setting 3, 50% duty cycle on a Branson Sonifier 450 with microtip. Extracts were incubated for 5 h at 4°C with GammaBind G Sepharose that was prebound with mouse anti-hnRNP K (3C2; Santa Cruz) or mouse anti-tubulin (B7; Santa Cruz) antibody. Bound samples were washed three times for 10 min in binding buffer supplemented with 1 M urea and 0.5 M NaCl and then resuspended in 50 mM Tris (pH 6.3), 5 mM EDTA, 1% SDS, and 10 mM DTT. Cross-links were reversed by heating for 45 min at 70°C.

The primary antibodies used for immunoblots were goat anti-cyclin T1 (T-18; Santa Cruz), mouse anti-CDK9 (D-7; Santa Cruz), chicken anti-HEXIM1 (ab37711; Abcam), mouse anti-hnRNP Q/R (I8E4; Abcam), and mouse anti-hnRNP K (3C2; Santa Cruz). The cyclin T1, CDK9, and hnRNP Q/R antibodies were used at 1:1000 dilution; the HEXIM1 antibody was used at 1:2000 dilution; and the hnRNP K antibody was used at 1:200 dilution. Nonspecific rabbit IgG (Sigma) was used at 1:10,000 dilution. The immunoblots in Figure 4, A and C, used horseradish peroxidase-conjugated goat anti-mouse (PharMingen) or donkey anti-goat (Santa Cruz) secondary antibodies and were developed with ECL+ (G.E. Biosciences) and imaged using Typhoon 9400. Other immunoblots used goat anti-mouse secondary conjugated to IR800CW dye (Rockland Immunochemicals), goat anti-chicken secondary conjugated to IR700 dye (Rockland Immunochemicals), or goat anti-rabbit secondary conjugated to Alexa Fluor 680 (Invitrogen) and were imaged on the Odyssey Infrared Imaging System (LI-COR).

RNAi

HeLa cells were transfected with siRNAs using Lipofectamine 2000 (Invitrogen), according to the manufacturer's instructions. Cells were split to new wells 48 h after initial transfection and transfected again 24 h later. All cells were harvested by trypsin 48 h after final transfection. The hnRNP K siRNA top-strand sequence was UAUUAAGGCUCUCCGUACAUU (Moumen et al. 2005). The negative control siRNA top-strand sequence was ACGCC CUUCUCAGUUAGGGTT.

ACKNOWLEDGMENTS

We thank Jamie Williamson for RAT tag discussion; David Peabody for the initial PP7 coat protein expression construct; Mark Mamula for human La antibody; Don Rio, Marco Blanchette, and Lori Kohlstaedt for assistance with mass spectrometry; and Dragony Fu for pcDNA 3.1 TAP vector construction. Specials thanks go to B. Andrew Stewart for his contributions to studies of B2 RNA. Funding for this project was provided by the University of California Cancer Research Coordinating Committee.

Received March 2, 2007; accepted March 23, 2007.

REFERENCES

Allen, T.A., Von Kaenel, S., Goodrich, J.A., and Kugel, J.F. 2004. The SINE-encoded mouse B2 RNA represses mRNA transcription in response to heat shock. *Nat. Struct. Mol. Biol.* **11:** 816–821.

Ausubel, F., Brent, R., Kingston, R., Moore, D., Seidman, F., Smith, J., and Struhl, K. 1996. *Current protocols in molecular biology*. Wiley, New York.

Bachler, M., Schroeder, R., and von Ahsen, U. 1999. StreptoTag: A novel method for the isolation of RNA-binding proteins. *RNA* **5:** 1509–1516.

Bardwell, V.J. and Wickens, M. 1990. Purification of RNA and RNA–protein complexes by an R17 coat protein affinity method. *Nucleic Acids Res.* **18:** 6587–6594.

Bertone, P., Gerstein, M., and Snyder, M. 2005. Applications of DNA tiling arrays to experimental genome annotation and regulatory pathway discovery. *Chromosome Res.* **13:** 259–274.

Blencowe, B.J. 2002. Transcription: Surprising role for an elusive small nuclear RNA. *Curr. Biol.* **12:** R147–R149.

Bomsztyk, K., Denisenko, O., and Ostrowski, J. 2004. hnRNP K: One protein, multiple processes. *Bioessays* **26:** 629–638.

Carey, J. and Uhlenbeck, O.C. 1983. Kinetic and thermodynamic characterization of the R17 coat protein–ribonucleic acid interaction. *Biochemistry* **22:** 2610–2615.

Carty, S.M. and Greenleaf, A.L. 2002. Hyperphosphorylated C-terminal repeat domain-associating proteins in the nuclear proteome link transcription to DNA/chromatin modification and RNA processing. *Mol. Cell. Proteomics* **1:** 598–610.

Chambers, J.C., Kurilla, M.G., and Keene, J.D. 1983. Association between the 7S RNA and the lupus La protein varies among cell types. *J. Biol. Chem.* **258:** 11438–11441.

Costa, F.F. 2005. Noncoding RNAs: New players in eukaryotic biology. *Gene* **357:** 83–94.

Czaplinski, K., Kocher, T., Schelder, M., Segref, A., Wilm, M., and Mattaj, I.W. 2005. Identification of 40LoVe, a *Xenopus* hnRNP D family protein involved in localizing a TGF-β-related mRNA during oogenesis. *Dev. Cell* **8:** 505–515.

Das, R., Zhou, Z., and Reed, R. 2000. Functional association of U2 snRNP with the ATP-independent spliceosomal complex E. *Mol. Cell* **5:** 779–787.

Egloff, S., Van Herreweghe, E., and Kiss, T. 2006. Regulation of polymerase II transcription by 7SK snRNA: Two distinct RNA elements direct P-TEFb and HEXIM1 binding. *Mol. Cell. Biol.* **26:** 630–642.

Eliceiri, G.L. 2006. The vertebrate E1/U17 small nucleolar ribonucleoprotein particle. *J. Cell. Biochem.* **98:** 486–495.

Eng, J.K., McCormack, A.L., and Yates, J.R. 1994. An approach to correlate tandem mass spectral data of peptides with amino acid sequences in a protein database. *J. Am. Soc. Mass Spectrom.* **5:** 976–989.

Espinoza, C.A., Allen, T.A., Hieb, A.R., Kugel, J.F., and Goodrich, J.A. 2004. B2 RNA binds directly to RNA polymerase II to repress transcript synthesis. *Nat. Struct. Mol. Biol.* **11:** 822–829.

Granneman, S., Vogelzangs, J., Luhrmann, R., van Venrooij, W.J., Pruijn, G.J., and Watkins, N.J. 2004. Role of pre-rRNA base pairing and 80S complex formation in subnucleolar localization of the U3 snoRNP. *Mol. Cell. Biol.* **24:** 8600–8610.

Hammond, S.M. 2006. MicroRNAs as oncogenes. *Curr. Opin. Genet. Dev.* **16:** 4–9.

Hartmuth, K., Urlaub, H., Vornlocher, H.P., Will, C.L., Gentzel, M., Wilm, M., and Luhrmann, R. 2002. Protein composition of human prespliceosomes isolated by a tobramycin affinity-selection method. *Proc. Natl. Acad. Sci.* **99:** 16719–16724.

Hartmuth, K., Vornlocher, H.P., and Luhrmann, R. 2004. Tobramycin affinity tag purification of spliceosomes. *Methods Mol. Biol.* **257:** 47–64.

Huttenhofer, A. and Vogel, J. 2006. Experimental approaches to identify noncoding RNAs. *Nucleic Acids Res.* **34:** 635–646.

Jurica, M.S. and Moore, M.J. 2002. Capturing splicing complexes to study structure and mechanism. *Methods* **28:** 336–345.

Kaneko, S. and Manley, J.L. 2005. The mammalian RNA polymerase II C-terminal domain interacts with RNA to suppress transcription-coupled 3′ end formation. *Mol. Cell* **20:** 91–103.

Kapust, R.B., Tozser, J., Fox, J.D., Anderson, D.E., Cherry, S., Copeland, T.D., and Waugh, D.S. 2001. Tobacco etch virus protease: Mechanism of autolysis and rational design of stable mutants with wild-type catalytic proficiency. *Protein Eng.* **14:** 993–1000.

Kinsella, T.M. and Nolan, G.P. 1996. Episomal vectors rapidly and stably produce high-titer recombinant retrovirus. *Hum. Gene Ther.* **7:** 1405–1413.

Kohno, K., Izumi, H., Uchiumi, T., Ashizuka, M., and Kuwano, M. 2003. The pleiotropic functions of the Y-box-binding protein, YB-1. *Bioessays* **25:** 691–698.

Krecic, A.M. and Swanson, M.S. 1999. hnRNP complexes: Composition, structure, and function. *Curr. Opin. Cell Biol.* **11:** 363–371.

Lamond, A.I. and Sproat, B.S. 1994. Isolation and characterization of ribonucleoprotein complexes. In *RNA processing* (ed. S.J. Higgins), pp. 103–140. IRL Press, Oxford.

LeCuyer, K.A., Behlen, L.S., and Uhlenbeck, O.C. 1995. Mutants of the bacteriophage MS2 coat protein that alter its cooperative binding to RNA. *Biochemistry* **34:** 10600–10606.

Li, Q., Price, J.P., Byers, S.A., Cheng, D., Peng, J., and Price, D.H. 2005. Analysis of the large inactive P-TEFb complex indicates that it contains one 7SK molecule, a dimer of HEXIM1 or HEXIM2, and two P-TEFb molecules containing Cdk9 phosphorylated at threonine 186. *J. Biol. Chem.* **280:** 28819–28826.

Liang, X.H. and Fournier, M.J. 2006. The helicase Has1p is required for snoRNA release from pre-rRNA. *Mol. Cell. Biol.* **26:** 7437–7450.

Lim, F. and Peabody, D.S. 2002. RNA recognition site of PP7 coat protein. *Nucleic Acids Res.* **30:** 4138–4144.

Lim, F., Downey, T.P., and Peabody, D.S. 2001. Translational repression and specific RNA binding by the coat protein of the *Pseudomonas* phage PP7. *J. Biol. Chem.* **276:** 22507–22513.

Lingner, J. and Cech, T.R. 1996. Purification of telomerase from *Euplotes aediculatus*: Requirement of a primer 3′ overhang. *Proc. Natl. Acad. Sci.* **93:** 10712–10717.

Makeyev, A.V. and Liebhaber, S.A. 2002. The poly(C)-binding proteins: A multiplicity of functions and a search for mechanisms. *RNA* **8:** 265–278.

Mattick, J.S. and Makunin, I.V. 2006. Noncoding RNA. *Hum. Mol. Genet.* **15:** R17–R29.

Michels, A.A., Nguyen, V.T., Fraldi, A., Labas, V., Edwards, M., Bonnet, F., Lania, L., and Bensaude, O. 2003. MAQ1 and 7SK RNA interact with CDK9/cyclin T complexes in a transcription-dependent manner. *Mol. Cell. Biol.* **23:** 4859–4869.

Mitchell, J.R., Cheng, J., and Collins, K. 1999a. A box H/ACA small nucleolar RNA-like domain at the human telomerase RNA 3′ end. *Mol. Cell. Biol.* **19:** 567–576.

Mitchell, J.R., Wood, E., and Collins, K. 1999b. A telomerase component is defective in the human disease dyskeratosis congenita. *Nature* **402:** 551–555.

Morgenstern, J.P. and Land, H. 1990. Advanced mammalian gene transfer: High titer retroviral vectors with multiple drug selection markers and a complementary helper-free packaging cell line. *Nucleic Acids Res.* **18:** 3587–3596.

Moumen, A., Masterson, P., O'Connor, M.J., and Jackson, S.P. 2005. hnRNP K: An HDM2 target and transcriptional coactivator of p53 in response to DNA damage. *Cell* **123:** 1065–1078.

Mourelatos, Z., Abel, L., Yong, J., Kataoka, N., and Dreyfuss, G. 2001. SMN interacts with a novel family of hnRNP and spliceosomal proteins. *EMBO J.* **20:** 5443–5452.

Nguyen, V.T., Kiss, T., Michels, A.A., and Bensaude, O. 2001. 7SK small nuclear RNA binds to and inhibits the activity of CDK9/cyclin T complexes. *Nature* **414:** 322–325.

Niranjanakumari, S., Lasda, E., Brazas, R., and Garcia-Blanco, M.A. 2002. Reversible cross-linking combined with immunoprecipitation to study RNA–protein interactions in vivo. *Methods* **26:** 182–190.

Noller, H.F. 2004. The driving force for molecular evolution of translation. *RNA* **10:** 1833–1837.

Peterlin, B.M. and Price, D.H. 2006. Controlling the elongation phase of transcription with P-TEFb. *Mol. Cell* **23:** 297–305.

Puig, O., Caspary, F., Rigaut, G., Rutz, B., Bouveret, E., Bragado-Nilsson, E., Wilm, M., and Séraphin, B. 2001. The tandem affinity purification (TAP) method: A general procedure of protein complex purification. *Methods* **24:** 218–229.

Ridanpaa, M., van Eenennaam, H., Pelin, K., Chadwick, R., Johnson, C., Yuan, B., vanVenrooij, W., Pruijn, G., Salmela, R., Rockas, S., et al. 2001. Mutations in the RNA component of RNase MRP cause a pleiotropic human disease, cartilage–hair hypoplasia. *Cell* **104:** 195–203.

Rigaut, G., Shevchenko, A., Rutz, B., Wilm, M., Mann, M., and Seraphin, B. 1999. A generic protein purification method for protein complex characterization and proteome exploration. *Nat. Biotechnol.* **17:** 1030–1032.

Rinke, J. and Steitz, J.A. 1982. Precursor molecules of both human 5S ribosomal RNA and transfer RNAs are bound by a cellular protein reactive with anti-La lupus antibodies. *Cell* **29:** 149–159.

Sano, M., Abdellatif, M., Oh, H., Xie, M., Bagella, L., Giordano, A., Michael, L.H., DeMayo, F.J., and Schneider, M.D. 2002. Activation and function of cyclin T-Cdk9 (positive transcription elongation factor-b) in cardiac muscle-cell hypertrophy. *Nat. Med.* **8:** 1310–1317.

Schroeder, R., Barta, A., and Semrad, K. 2004. Strategies for RNA folding and assembly. *Nat. Rev. Mol. Cell Biol.* **5:** 908–919.

Shav-Tal, Y., Singer, R.H., and Darzacq, X. 2004. Imaging gene expression in single living cells. *Nat. Rev. Mol. Cell Biol.* **5:** 855–861.

Singh, R. and Valcarcel, J. 2005. Building specificity with nonspecific RNA-binding proteins. *Nat. Struct. Mol. Biol.* **12:** 645–653.

Srisawat, C. and Engelke, D.R. 2001. Streptavidin aptamers: Affinity tags for the study of RNAs and ribonucleoproteins. *RNA* **7:** 632–641.

Srisawat, C. and Engelke, D.R. 2002. RNA affinity tags for purification of RNAs and ribonucleoprotein complexes. *Methods* **26:** 156–161.

Tabb, D.L., McDonald, W.H., and Yates III, J.R. 2002. DTASelect and Contrast: Tools for assembling and comparing protein identifications from shotgun proteomics. *J. Proteome Res.* **1:** 21–26.

Tars, K., Fridborg, K., Bundule, M., and Liljas, L. 2000. The three-dimensional structure of bacteriophage PP7 from *Pseudomonas aeruginosa* at 3.7-Å resolution. *Virology* **272:** 331–337.

Thiel, C.T., Horn, D., Zabel, B., Ekici, A.B., Salinas, K., Gebhart, E., Ruschendorf, F., Sticht, H., Spranger, J., Muller, D., et al. 2005. Severely incapacitating mutations in patients with extreme short stature identify RNA-processing endoribonuclease RMRP as an essential cell growth regulator. *Am. J. Hum. Genet.* **77:** 795–806.

Vulliamy, T., Marrone, A., Goldman, F., Dearlove, A., Bessler, M., Mason, P.J., and Dokal, I. 2001. The RNA component of telomerase is mutated in autosomal dominant dyskeratosis congenita. *Nature* **413:** 432–435.

Vulliamy, T.J., Marrone, A., Dokal, I., and Mason, P.J. 2002. Association between aplastic anemia and mutations in telomerase RNA. *Lancet* **359:** 2168–2170.

Walker, S.C. and Engelke, D.R. 2006. Ribonuclease P: The evolution of an ancient RNA enzyme. *Crit. Rev. Biochem. Mol. Biol.* **41:** 77–102.

Wang, Y. and Rando, R.R. 1995. Specific binding of aminoglycoside antibiotics to RNA. *Chem. Biol.* **2:** 281–290.

Wassarman, D.A. and Steitz, J.A. 1991. Structural analyses of the 7SK ribonucleoprotein (RNP), the most abundant human small RNP of unknown function. *Mol. Cell. Biol.* **11:** 3432–3445.

Watkins, N.J., Segault, V., Charpentier, B., Nottrott, S., Fabrizio, P., Bachi, A., Wilm, M., Rosbash, M., Branlant, C., and Luhrmann, R. 2000. A common core RNP structure shared between the small nucleoar box C/D RNPs and the spliceosomal U4 snRNP. *Cell* **103:** 457–466.

Yang, Z., Zhu, Q., Luo, K., and Zhou, Q. 2001. The 7SK small nuclear RNA inhibits the CDK9/cyclin T1 kinase to control transcription. *Nature* **414:** 317–322.

Yik, J.H., Chen, R., Nishimura, R., Jennings, J.L., Link, A.J., and Zhou, Q. 2003. Inhibition of P-TEFb (CDK9/Cyclin T) kinase and RNA polymerase II transcription by the coordinated actions of HEXIM1 and 7SK snRNA. *Mol. Cell* **12:** 971–982.

Zhou, Z., Licklider, L.J., Gygi, S.P., and Reed, R. 2002. Comprehensive proteomic analysis of the human spliceosome. *Nature* **419:** 182–185.